

Magnetic interactions and interface properties in Co/Fe multilayers

L. Agazzi

Department of Physics, University of Parma and INFN, 43100 Parma, Italy

S. Bennett

Department of Synchrotron Radiation, Daresbury Laboratory, Daresbury, Warrington Cheshire WA4 4AD, United Kingdom

F. J. Berry

Department of Chemistry, The Open University, Walton Hall, Milton Keynes, United Kingdom

M. Carbucicchio,^{a)} M. Rateo, and G. Ruggiero

Department of Physics, University of Parma and INFN, 43100 Parma, Italy

G. Turilli

MASPEC Laboratory, CNR, Parma, Italy

(Received 21 May 2001; accepted for publication 12 June 2002)

Co/Fe multilayers with different layer thickness formed by electron beam evaporation in ultrahigh vacuum have been investigated by grazing incidence x-ray reflectivity (GIXRR) and alternating gradient force magnetometry. The interface thicknesses are lower than GIXRR uncertainty (~ 1 nm), favoring a strong magnetic exchange interaction between the layers responsible for their single phase magnetic behavior. The hysteresis loops were interpreted as the result of two different magnetization processes related to the presence of an out-of-plane component of the magnetization.

© 2002 American Institute of Physics. [DOI: 10.1063/1.1499203]

I. INTRODUCTION

Modern permanent magnets are characterized by high coercive fields resulting from strong magnetocrystalline anisotropy. Additionally, permanent magnet materials require high saturation magnetizations and high Curie temperatures. However, the achievement of these different characteristics in a unique phase is very difficult. The best way to overcome this problem is to combine the concepts of composite (i.e., a system constituted by different phases but exhibiting a single phase behavior) and nanostructure (i.e., system composed of finely distributed particles of nanometric dimensions). The objective is to obtain nanostructured materials formed by exchange coupled soft and hard magnetic phases on a nanometric scale, but showing single phase magnetic behavior.^{1,2} This coupling can lead to remanence and energy product enhancement, thus providing new materials with superior permanent magnet characteristics. Such materials have potential application in high quality performance devices in the fields of magnetoelectronics, high density magnetic recording materials, sensor devices, and microsystem technology.

One way of preparing nanocomposite materials is to grow them in the form of multilayers where soft and hard magnetic materials are intercalated. This permits a high degree of control and reproducibility of both structure and properties. Although the feasibility of planar magnetic nanocomposites has been demonstrated, many difficulties continue to exist,³⁻⁵ and in particular (i) those related to the interface properties (i.e., roughness, structure, and nature)

which can influence the exchange coupling between the layers,^{2,6} and (ii) those related to the obtainment of single phases and easy axis alignment for the hard component.⁴

Using simple materials (i.e., iron and cobalt) and ultrahigh vacuum e-beam deposition technique we demonstrated the feasibility of planar magnetic nanocomposites involving a dominant soft phase and showing a magnetic energy density superior to that of the hard component.^{7,8} It was supposed that, in addition to the high purity of the components and the thickness of the layers (chosen in the range of the exchange length), the high quality of the obtained interfaces allowed the strong exchange coupling between the ferromagnetic phases.

Co/Fe interfaces have been largely studied for both sputtered and epitaxially grown multilayers. It has been found that interdiffusion phenomena with formation of Co-Fe phases at the interfaces causes the arising of stress states, which, in turn, influence the magnetic anisotropy of the multilayer.⁹ The study of Co/Fe bilayers showed that the deposition order (i.e., Co on Fe or Fe on Co) strongly influences the morphology of the interfaces and dramatically changes the coercivity of the system.¹⁰ The dependence of cobalt structure on the Co layer thickness, and the cluster formation, was also studied in epitaxially grown Co/Fe multilayers.¹¹

In the present work *e*-beam deposited Co/Fe multilayers have been studied by grazing incidence x-ray reflectivity and alternating gradient force magnetometry. The nature, thickness, and morphology of the interfaces have been correlated to the magnetic interactions arising between the layers and the magnetization processes of the system.

^{a)}Electronic mail: carbucicchio@fis.unipr.it

II. EXPERIMENT

Co/Fe multilayers were formed by electron-beam evaporation in ultrahigh vacuum onto quartz substrates, carefully washed (acetone–trichloroethylene solution followed by an ultrasound bath in isopropyl alcohol). The starting vacuum was $\sim 10^{-8}$ Pa and the operating one $\sim 10^{-6}$ Pa. The deposition rates were 0.7 and 0.5 nm/min for Co and Fe, respectively. The film thickness was measured during deposition by a quartz microbalance. All samples were constituted by five bilayers of $\text{Co}_t/\text{Fe}_{3t}$ covered by a Co_t capping layer, with $t = 5.0, 10.0,$ and 15.0 nm. Both grazing incidence x-ray diffraction (GIXRD) and high energy electron diffraction (HEED) measurements revealed that analogous multilayers grown under the same conditions show a polycrystalline structure with hcp Co and bcc Fe. No preferred crystallographic orientations were detected.⁸

Grazing incidence x-ray reflectivity (GIXRR) measurements were performed on the Station 9.4 at Synchrotron Radiation Source (SRS) at Daresbury Laboratory at 298 K. The x-ray beam was focused with a Pt coated toroidal Si mirror. The beam size at the focal point was < 1 mm. A fixed exit double crystal monochromator provided a monochromatic x-ray beam which was detected by a solid state Ge detector. Because of the very similar refractive indices of Co and Fe, it was necessary to exploit the fact that the dispersive terms of the atomic scattering factors change rapidly in the vicinity of an absorption edge. In these measurements a point was chosen (1.746 \AA) just below the Fe K edge to enhance contrast while minimizing attenuation through the sample. The spectra were fitted using the Parratt algorithm¹² with the Nevot–Croce correction.¹³

All magnetic measurements were carried out at room temperature by means of an alternating gradient force magnetometer (AGFM). The full scale sensitivity was better than 10^{-8} emu.

Both initial magnetization (M_I) curves on as-deposited samples and hysteresis loops were measured applying the magnetic field of up to 20 kOe in the film plane.

The magnetic interaction between the layers was studied by means of the ΔM -plot technique.¹⁴ The *interaction-based deviation parameter* $\Delta M(H)$ is defined as:

$$\Delta M(H) = I_{\text{DCD}}(H) - [1 - 2I_{\text{IRM}}(H)],$$

where $I_{\text{IRM}}(H)$ is the *isothermal remanence* curve and $I_{\text{DCD}}(H)$ is the dc *demagnetization remanence* curve, both normalized to the saturation remanence magnetization. The $I_{\text{IRM}}(H)$ is obtained applying an increasing magnetic field to the demagnetized multilayers, and plotting the remanence after removing the field. The $I_{\text{DCD}}(H)$ is obtained by plotting the remanence after a progressive demagnetization from a previously saturated state at 1 kOe.

For noninteracting assemblies of uniaxial particles, ΔM is zero at any value of applied field. Deviations of ΔM from zero in real materials are interpreted as being due to magnetic interactions. A measurement of ΔM thus gives a fingerprint of magnetic interactions in a medium. Positive values of ΔM are due to interactions promoting the magnetized

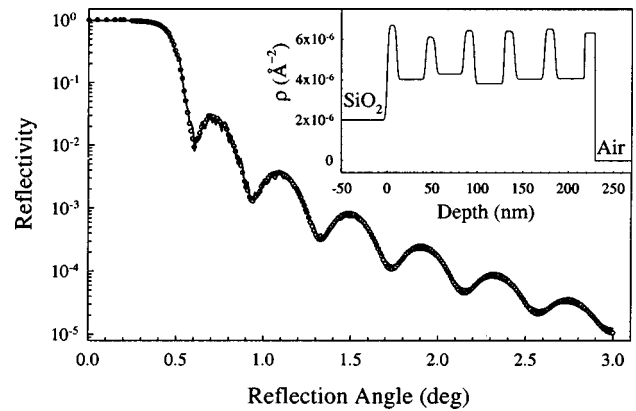


FIG. 1. Grazing incidence x-ray reflectivity (GIXRR) pattern for the $\text{Co}_{10.0 \text{ nm}}/\text{Fe}_{30.0 \text{ nm}}$ multilayer (open circles: the experimental data, and continuous line: the best fit). The profile of the scattering length density ρ is also shown (inset).

state, while negative values of ΔM are caused by interactions tending to assist magnetization reversal.¹⁵

For all samples, the differential of the remanence curves, calculated from smoothed data applying the Loess algorithm, can be directly related to the switching field distributions (SFD) of the system:

$$\text{SFD}(H) = \left(\frac{dM(H)}{dH} \right) \cdot \frac{1}{H_C},$$

where $\text{SFD}(H)dH$ is the fraction of magnetic particles and domains reversing their moments in the field range from H to $H+dH$.

III. RESULTS AND DISCUSSION

Figure 1 shows the grazing incidence x-ray reflectivity (GIXRR) pattern for the $\text{Co}_{10.0 \text{ nm}}/\text{Fe}_{30.0 \text{ nm}}$ multilayer. The fitting of the experimental data (Fig. 1) was performed using the scattering length density profile shown in the inset. The values of the thickness of both the Co and Fe layers were in good agreement with those measured by the quartz microbalance during evaporation. Moreover, the Co and Fe densities were found to be only $\sim 1\%$ lower than those of the corresponding bulk elements. Tacking into account the Co and Fe layer thickness, the fitting of the data gives an average value of the interface thickness (~ 1 nm) comparable with the limit of the GIXRR technique. In these conditions, the separation between contributions from roughness and interdiffusion zone was inhibited.

These results agree with surface Mössbauer analysis of Co/Fe multilayers which have been electron beam evaporated under identical conditions in ultrahigh vacuum.¹⁶ In order to increase the interface contribution, very thin ^{57}Fe layers were evaporated. The hyperfine magnetic field distribution obtained from the fitting of the Mössbauer spectra indicated that a sharp Fe concentration gradient has been formed at the interface. However, from the results it was impossible to distinguish between an abrupt transition from Fe to Co at the interface, and a very thin interfacial region (~ 0.7 nm thick) constituted by FeCo alloy.

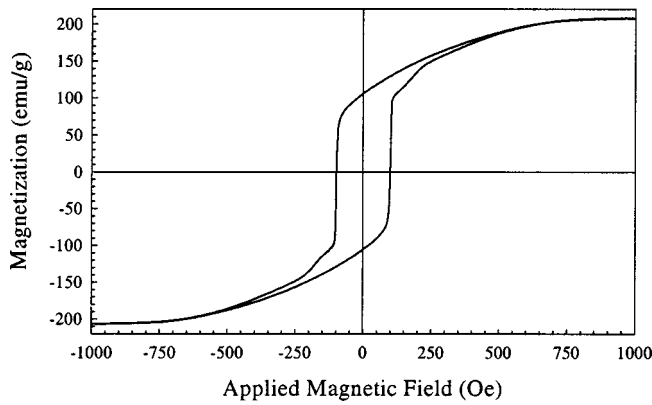


FIG. 2. Hysteresis loop for the $\text{Co}_{10.0 \text{ nm}}/\text{Fe}_{30.0 \text{ nm}}$ multilayer.

The hysteresis loop for the $\text{Co}_{10.0 \text{ nm}}/\text{Fe}_{30.0 \text{ nm}}$ multilayer is reported in Fig. 2. The remanence ratio is equal to 0.5 and the loop has a narrow hysteretic tail up to ~ 450 Oe. The value of saturation magnetization is close to that of iron, i.e., the soft phase, and the coercive field is comparable with that of a 10.0 nm thick cobalt single film, deposited under the same conditions.⁷

Figure 3 shows the initial magnetization (M_I) and the isothermal remanence magnetization (I_{IRM}) curves for the same sample.

The magnetization initially increases from the ac demagnetization state along a straight line, then there is a dramatic change at the coercive field value (H_c) followed by a continuous variation in the slope up to the saturation value. The initial magnetization is reversible up to ~ 50 Oe ($I_{\text{IRM}} = 0$), irreversible from ~ 50 Oe to H_c , and then reversible up to saturation.

Magnetic force microscopy studies of $\text{Co}_{10.0 \text{ nm}}/\text{Fe}_{30.0 \text{ nm}}$ grown under the same conditions have shown the presence of very regular long and parallel domain regions (*stripe domains*).¹⁷ This implies that magnetization has a component perpendicular to the film plane pointing up and down alternately and, from line intensity ratios of conversion electron Mössbauer spectra, an $\sim 45^\circ$ out-of-plane angle of the magnetization direction was determined.

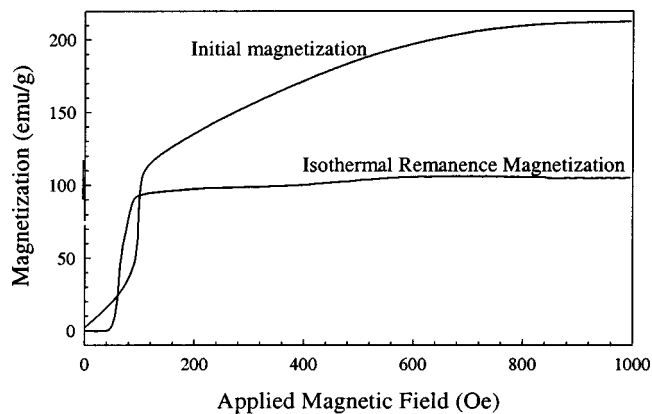


FIG. 3. Initial magnetization $M_I(H)$ and isothermal remanence magnetization $I_{\text{IRM}}(H)$ curves for the $\text{Co}_{10.0 \text{ nm}}/\text{Fe}_{30.0 \text{ nm}}$ multilayer.

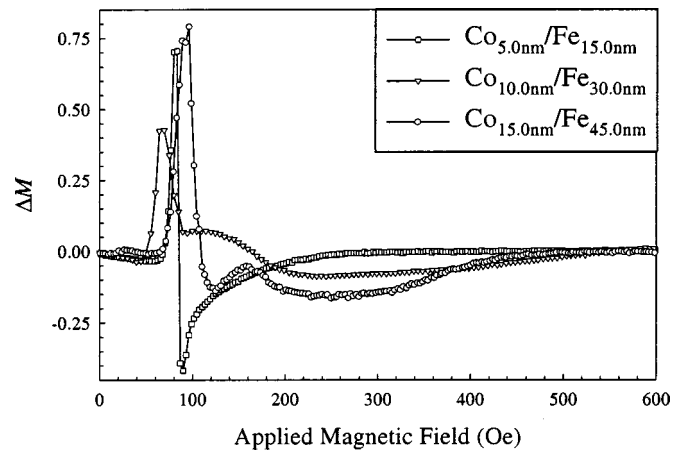


FIG. 4. ΔM plot for Co/Fe multilayers.

On the basis of these results, the hysteresis loop (Fig. 2) carried out applying the field parallel to the film plane, can be interpreted as the result of two magnetization processes: (i) a process at low applied fields due to the domain wall motion which produces the alignment of the in-plane magnetization component, and (ii) a rotation at higher applied fields of the perpendicular magnetization component into the film plane.¹⁸ It is worth noting that a residual domain wall motion persisting up to ~ 450 Oe is also responsible for the observed narrow tail of the loop. The last interpretation is in good agreement with the I_{IRM} curve (Fig. 3) that shows, in applied fields ranging between 50 and 450 Oe, a behavior typical of irreversible magnetization processes.

Similar results were obtained for $\text{Co}_{5.0 \text{ nm}}/\text{Fe}_{15.0 \text{ nm}}$ and $\text{Co}_{15.0 \text{ nm}}/\text{Fe}_{45.0 \text{ nm}}$. All multilayers therefore show an enhanced magnetic energy density, having the saturation magnetization close to that of the soft component and the coercive field comparable with that of the hard one.

The magnetic behavior for all samples is typical of a single magnetic phase. In fact:

(1) The magnetization curves (see, for example, Fig. 2) cannot be explained as the addition of distinct iron and cobalt hysteresis loops, which are characterized by low and high coercive fields (H_c) respectively. This would give rise to a step in correspondence to the lower H_c value in the second quadrant.

(2) The well defined stripe domain structure shown by all samples¹⁷ cannot be interpreted as due to independent magnetic phases. Indeed, independent magnetic phases would give rise to domain structures characterized by different size and different direction of the magnetization vector.

The single phase magnetic behavior of these multilayers suggests the presence of strong magnetic interactions between the layers.

Figure 4 shows the ΔM -plots for the $\text{Co}_{5.0 \text{ nm}}/\text{Fe}_{15.0 \text{ nm}}$, $\text{Co}_{10.0 \text{ nm}}/\text{Fe}_{30.0 \text{ nm}}$ and $\text{Co}_{15.0 \text{ nm}}/\text{Fe}_{45.0 \text{ nm}}$ multilayers. The high positive value of ΔM for applied fields up to H_c is strongly indicative of a ferromagnetic interaction (exchange coupling) between the layers.

The $\Delta M(H)$ curve for $\text{Co}_{5.0 \text{ nm}}/\text{Fe}_{15.0 \text{ nm}}$ shows the sharpest transition from positive to negative values. Since the slope of this transition can be linked to the strength of the

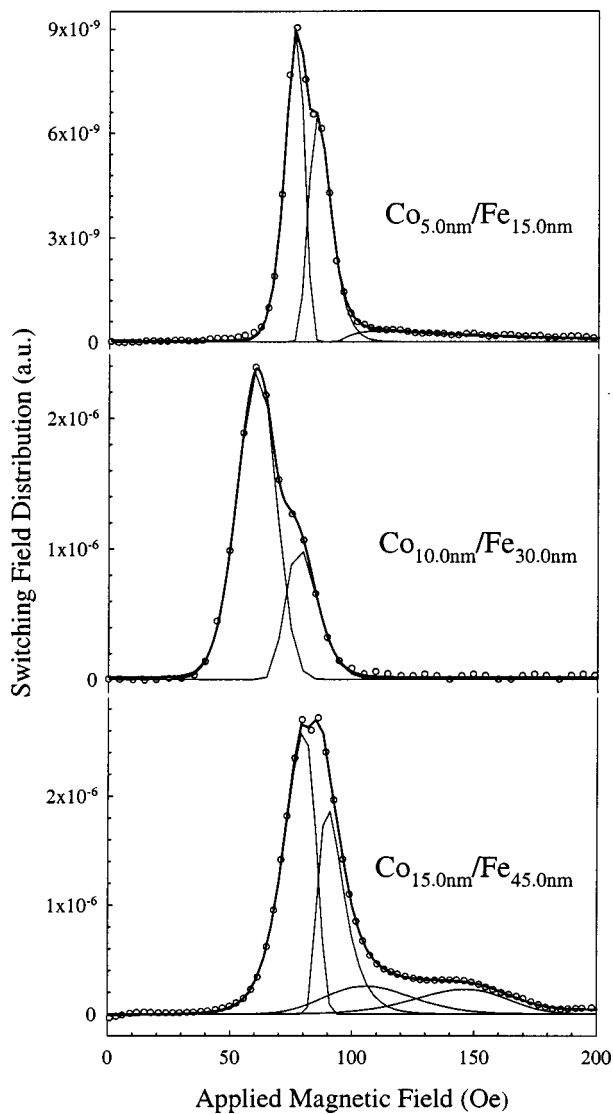


FIG. 5. Remanence switching field distributions (SFD) for Co/Fe multilayers.

exchange interaction,¹⁹ this sample is therefore the strongest magnetically coupled multilayer, as might be expected from the thinner iron layer.

Figure 5 shows the switching field distributions for $\text{Co}_{5.0\text{ nm}}/\text{Fe}_{15.0\text{ nm}}$, $\text{Co}_{10.0\text{ nm}}/\text{Fe}_{30.0\text{ nm}}$ and $\text{Co}_{15.0\text{ nm}}/\text{Fe}_{45.0\text{ nm}}$ multilayers obtained by differentiating the $I_{\text{IRM}}(H)$ curves. The distance between the two main peaks of the fitting is inversely related to the exchange coupling stiffness.²⁰ From

the figure it follows that all samples are strongly magnetically coupled with, again, $\text{Co}_{5.0\text{ nm}}/\text{Fe}_{15.0\text{ nm}}$, being the strongest coupled multilayer.

IV. CONCLUSIONS

From the analysis performed on the Co/Fe multilayers electron beam evaporated under ultrahigh vacuum, the following conclusions can be drawn:

(1) Co and Fe densities are only $\sim 1\%$ lower than those of the corresponding bulk elements. The thickness of the interfaces are lower than the GIXRR uncertainty, which is ~ 1 nm in the case of the analyzed layers.

(2) The soft and hard magnetic phases are exchange coupled giving rise to planar nanocomposites showing single phase magnetic behavior.

(3) The in-plane hysteresis loops result from two different magnetization processes, one due to domain wall movement and the other to coherent rotation of the magnetization vector showing an out-of-plane component.

(4) Different experimental approaches demonstrate that the strongest exchange coupled stiffness is obtained in the sample with the thinnest iron layers.

¹R. Skomski, J. Appl. Phys. **76**, 7059 (1994).

²I. A. Al-Omari and D. J. Sellmyer, Phys. Rev. B **52**, 3441 (1995).

³E. E. Fullerton, J. S. Jiang, M. Grimsditch, C. H. Sowers, and S. D. Bader, Phys. Rev. B **58**, 12193 (1998).

⁴S. Parhofer, G. Giert, J. Wecker, and L. Schultz, IEEE Trans. Magn. **32**, 4437 (1996).

⁵M. Shindo, M. Ishizane, A. Sakuma, M. Kato, and T. Miyazahi, J. Appl. Phys. **81**, 4444 (1997).

⁶C. J. Yang and E. B. Park, J. Magn. Magn. Mater. **166**, 243 (1997).

⁷G. Asti, M. Carbuicchio, M. Rateo, and M. Solzi, J. Magn. Magn. Mater. **196-197**, 59 (1999).

⁸G. Asti, M. Carbuicchio, M. Ghidini, M. Rateo, G. Ruggiero, M. Solzi, F. D'Orazio, and F. Lucari, J. Appl. Phys. **87**, 6689 (2000).

⁹F. W. A. Dirne and C. J. M. Denissen, J. Magn. Magn. Mater. **78**, 122 (1989).

¹⁰M. H. Park, Y. K. Hong, S. H. Gee, M. L. Mottern, and T. W. Jang, J. Appl. Phys. **91**, 7218 (2002).

¹¹J. P. Jay, E. Jędryka, M. Wójcik, J. Dekoster, G. Langouche, and P. Panisod, Z. Phys. B: Condens. Matter **101**, 329 (1996).

¹²L. G. Parratt, Phys. Rev. **95**, 359 (1954).

¹³L. Nevot and P. Croce, Rev. Phys. Appl. **15**, 761 (1980).

¹⁴P. E. Kelly, K. O'Grady, P. I. Mayo, and R. W. Chantrell, IEEE Trans. Magn. **25**, 3881 (1989).

¹⁵X.-D. Che and H. N. Bertram, J. Magn. Magn. Mater. **116**, 121 (1992).

¹⁶M. Carbuicchio and M. Rateo, Hyper. Interact. (in press).

¹⁷G. Ausanio, V. Iannotti, L. Lanotte, M. Carbuicchio, and M. Rateo, J. Magn. Magn. Mater. **226-230**, 1740 (2001).

¹⁸A. Hubert and R. Schäfer, *Magnetic Domains* (Springer, Berlin, 1998).

¹⁹I. A. Beardsley and J.-G. Zhu, IEEE Trans. Magn. **27**, 5037 (1991).

²⁰H. Göktürk and K. Maki, J. Magn. Magn. Mater. **167**, 166 (1997).

Journal of Applied Physics is copyrighted by the American Institute of Physics (AIP). Redistribution of journal material is subject to the AIP online journal license and/or AIP copyright. For more information, see <http://ojps.aip.org/japo/japcr/jsp>
Copyright of Journal of Applied Physics is the property of American Institute of Physics and its content may not be copied or emailed to multiple sites or posted to a listserv without the copyright holder's express written permission. However, users may print, download, or email articles for individual use.